6-1-2009

Measurement Of Drug-Protein Dissociation Rates By High-Performance Affinity Chromatography And Peak Profiling

John E Schiel
University of Nebraska - Lincoln

Corey M. Ohnmacht
University of Nebraska - Lincoln

David S. Hage
University of Nebraska-Lincoln, dhage1@unl.edu

Published in final edited form as:
Anal Chem. 2009 June 1; 81(11): 4320–4333. doi:10.1021/ac9000404.

MEASUREMENT OF DRUG-PROTEIN DISSOCIATION RATES BY HIGH-PERFORMANCE AFFINITY CHROMATOGRAPHY AND PEAK PROFILING

John E. Schiel, **Corey M. Ohnmacht**, and **David S. Hage***
Department of Chemistry, University of Nebraska-Lincoln, Lincoln, Nebraska 68588-0304

Abstract

The rate at which a drug or other small solute interacts with a protein is important in understanding the biological and pharmacokinetic behavior of these agents. One approach that has been developed for examining these rates involves the use of high-performance affinity chromatography (HPAC) and estimates of band-broadening through peak profiling. Previous work with this method has been based on a comparison of the statistical moments for a retained analyte versus non-retained species at a single, high flow rate to obtain information on stationary phase mass transfer. In this study an alternative approach was created that allows a broad range of flow rates to be used for examining solute-protein dissociation rates. Chromatographic theory was employed to derive equations that could be used with this approach on a single column, as well as with multiple columns to evaluate and correct for the impact of stagnant mobile phase mass transfer. The interaction of L-tryptophan with human serum albumin was used as a model system to test this method. A dissociation rate constant of 2.7 (± 0.2) s^{-1} was obtained by this approach at pH 7.4 and 37°C, which was in good agreement with previous values determined by other methods. The techniques described in this report can be applied to other biomolecular systems and should be valuable for the determination of drug-protein dissociation rates.

INTRODUCTION

The binding of drugs with proteins can be studied by many techniques, such as equilibrium dialysis, microdialysis, ultrafiltration, and various chromatographic methods.[1–13] The association equilibrium constants and degree of binding that are measured using these techniques are useful in helping to describe the transport and pharmacokinetics of drugs in the body.[14] For instance, human serum albumin (HSA) is a major serum protein in humans that is responsible for binding and transporting numerous drugs in blood.[15] It is known that the kinetics of such an interaction can play a significant role in the distribution, half life and activity of a given drug or hormone.[16, 17]

In the case of drug-protein binding in serum, it is generally assumed that the overall extent of protein binding is important and that the resulting free, or unbound, fraction of a drug is the biologically-active form (i.e., a model known as the “free drug hypothesis”).[18,19] However, there are some cases in which the free form of a drug does not directly correlate with its tissue uptake or bioavailability.[16,17,20–28] This has led to some competing models to describe drug delivery and uptake, such as those that incorporate receptor-mediated transport of drugs that are bound to specific serum proteins[23, 25] or those in which the rate of a drug/protein interaction falls in a range that can contribute to deviations from the free drug hypothesis.[16, 17, 24, 27] Rate constant measurements for these interactions are needed to

*Author for correspondence. Phone: (402) 472-2744; FAX: (402) 472-9402; dhage@unlserve.unl.edu.

compare these models, to determine when the free drug fraction is important, and to better predict the *in vivo* behavior that would be expected for a drug.[29] In addition, measurements of both the extent and rate of drug binding to serum proteins could be valuable in the screening of new drug candidates and in the design of improved analytical methods for determining the biologically-active fractions of drugs and other solutes in biological samples.[30–36]

Previous analytical techniques for examining the kinetics of drug-protein interactions have included stopped-flow analysis,[37–40] surface plasmon resonance (SPR),[35] microdialysis,[29] and various affinity chromatographic methods.[11,41–51] Stopped-flow techniques are limited to cases in which a suitable change in a spectroscopic signal is available to study a given drug-protein interaction.[37] SPR is commonly used in studying the kinetics of biomolecular systems; however, it has seen only very limited use for studying the rate of drug interactions with HSA and other serum proteins.[35] It has been suggested this lack of applications for SPR in this area is partly due to the relatively fast association/dissociation processes that are often present in the interactions of drugs with serum proteins like HSA.[29,45,51] Another problem in the use of SPR with these systems is that it can be difficult to obtain accurate data for weak binding by low mass drugs with limited solubility because the signal in SPR is proportional to the analyte's concentration, mass, and affinity for the immobilized ligand.[35] The microdialysis method has recently been adapted for use in examining the kinetics of drug-protein binding but requires HPLC for the later separation and measurement of drug in the dialysate, which can limit the throughput of this approach. This method also requires the careful selection of appropriate conditions for kinetic studies and makes use of non-linear curve fitting methods.[29] Past work using affinity chromatography and HPAC to examine the kinetics of drug-protein interactions[11, 41–51] and other systems of biological interest[52–54] has involved techniques based on plate height or band-broadening measurements,[31–48,50–54] and peak decay analysis.[49,50] Of these two approaches, the use of plate height or band-broadening measurements has received the most attention as a means for examining the rates of solute-ligand interactions.[41–48,50–54]

One variation on the band-broadening measurement approach is a method that has recently been referred to as "peak profiling".[11] The concept of peak profiling goes back to 1975, when expressions were derived for the first and second moments for an eluting analyte peak that could be used to calculate the dissociation rate constant for this analyte from an immobilized ligand based on the observed profiles for both the analyte and a non-retained species.[55] This approach was first used with low-performance supports and measurements made at a single flow rate to study the self-association of bovine neurophysin II and the binding of this agent with the neuropeptide Arg^8-vasopressin.[56–58] A mathematically equivalent approach was later used to study the rate of interaction of sugars with immobilized concanavalin A.[53] However, these methods gave values that were later thought to be underestimated due to either the presence of significant sources of band-broadening other than stationary phase mass transfer[56–58] or the possible presence of non-linear elution conditions (i.e., concentration-dependent behavior).[53,54] The method of peak profiling was recently examined again by using it with measurements conducted at single linear velocities and high flow rates to increase the relative contribution of "kinetic" broadening to the measured peak variances.[11] Although the results gave reasonably good agreement with those expected for a model system, this method did assume that there was no sample size dependence in the measured variances and that no major contributions to bandbroadening other than stationary phase mass transfer were present at the flow rate that was used for the kinetic studies.[11]

The use of peak profiling or a related method for rapidly determining solute-protein dissociation rate constants could be a valuable tool for determining and modeling the

expected kinetics of these interactions for potential drug candidates.[17,33,34] In this current paper, an alternative approach based on this technique, as illustrated in Figure 1, is described and explored for use in such studies. In this method, the analyte of interest and a non-retained solute are injected at several flow rates onto an affinity column under conditions where retention is independent of concentration (e.g., linear elution conditions). The observed peaks are then fit to an exponentially-modified Gaussian (EMG) model[59] (e.g., a Gaussian model with an additional exponential decay function) to give the first and second moments for the analyte and nonretained solute peaks. An equation derived from chromatographic theory is described and used to analyze these results through linear regression. Equations will also be developed to determine the effects of stationary phase mass transfer in such measurements when the experiment is performed on multiple columns. This approach is tested and evaluated by using the binding of L-tryptophan with HSA as a model system, making it possible to compare the results of this work with those obtained through previously-described techniques based on peak profiling or plate height measurements.[11, 51] The method presented in this report is a general one that should be useful in examining a variety of other biological interactions, including drug-protein binding.

THEORY

General Model

The binding of a drug or small solute with a protein like HSA is often described by the following reversible interaction.[3]

$$A+P \underset{k_d}{\overset{k_a}{\rightleftharpoons}} AP \tag{1}$$

$$K_a = \frac{k_a}{k_d} \tag{2}$$

The association equilibrium constant (K_a) for this system is given in eq 2 by the ratio of the second-order association rate constant (k_a) and the first-order dissociation rate constant (k_d). Peak profiling and band-broadening methods seek to determine kinetic values for a system like the one in eq 1 by passing a small plug of solute A through a column that contains an immobilized form of protein or ligand P. The first and second statistical moments for the resulting sample peak are measured and used to describe the retention and band-broadening of A, respectively. The second moment is then related to the kinetics of the interaction between A and P, after correcting for other sources of band-broadening in the column.[50]

The contributions to band-broadening that can occur as A passes through a column containing P include mobile phase mass transfer and eddy diffusion (as described collectively by the plate height term H_m), longitudinal diffusion (H_l), stagnant mobile phase mass transfer (H_{sm}), and stationary phase mass transfer (H_k).[50] These plate height terms are commonly viewed as being additive in nature and together make up the total observed plate height, H_{tot}. It is expected from these terms that varying the flow rate or linear velocity for a given separation will affect the retention and broadening of an eluting peak, as shown in Figure 2. When peak profiling is performed at a single flow rate, it has been suggested that it is desirable to increase the flow rate to obtain a condition in which the “kinetic” contribution to the band-broadening dominates (i.e., stationary phase mass transfer is a major component of band-broadening).[11] Under such conditions, it has been further suggested that eq 3 can be used to calculate k_d,

$$k_d = \frac{2 \cdot t_M^2 \cdot t_R - t_M}{\sigma_R^2 \cdot t_M^2 - \sigma_M^2 \cdot t_R^2} \quad (3)$$

where t_R and σ_R^2 are the retention time and variance of the peak for the injected analyte (with σ_R being the corresponding standard deviation), while t_M and σ_M^2 are the void time and variance of the peak (with a standard deviation of σ_M) for a non-retained solute under equivalent column and flow rate conditions.[11, 55] One assumption made in eq 3 is that all band-broadening contributions other than stationary phase mass transfer are the same for the retained and non-retained solutes. The effect of deviations from this assumption will be discussed later in this section.

Peak Profiling at a Single Flow Rate

In recent work using peak profiling at a single flow rate (or single linear velocity), two terms were used to identify an appropriate flow rate at which dissociation kinetics could be determined for a given solute-protein interaction. The first of these two terms was the critical ratio (η), as defined by eq 4.[11]

$$\eta = \frac{\sigma_R / t_R}{\sigma_M / t_M} \quad (4)$$

It can be shown that this ratio can also be written as given in eq 5,

$$\eta^2 = \frac{H_R}{H_M} \quad (5)$$

where H_R is the total plate height measured for a retained solute and H_M is the total plate height measured under the same conditions for a non-related solute. In a previous paper it has been suggested that peak profiling at a single flow rate should be performed under conditions in which the value of η is greater than one.[11] It can be seen from eq 5 that this situation occurs when $H_R > H_M$ and that η continues to increase as the difference in total plate height becomes larger for the retained versus non-retained solute.

To account for the dependence of plate height on linear velocity or flow rate, workers in Ref. 11 also derived a term called the “kinetic factor” (κ), which was defined as shown in eq 6.[11]

$$\kappa = \frac{\eta^2 - 1 \cdot \sigma_R^2 \cdot u}{\eta^2} \quad (6)$$

If eq 5 is inserted into this expression, the result is the following alternative form of eq 6.

$$\kappa = u\left(\sigma_R^2 - \frac{H_M}{H_R} \cdot \sigma_R^2\right) \quad (7)$$

If it is assumed that the only difference between H_R and H_M is due to stationary phase mass transfer, eq 7 indicates that κ is a measure of the total band-broadening of the retained peak, as represented by σ_R^2, versus the fraction of band-broadening that is not due to H_k, as given by $(H_M/H_R) \cdot \sigma_R^2$. It has been suggested in Ref. 11 that the value of κ should eventually level off as the linear velocity or flow rate is increased, thus indicating the conditions at which the kinetic contribution to band-broadening is maximized. Band-broadening measurements that are obtained at such a flow rate are then used along with eq 3 to

estimated k_d.[11] A dissociation rate constant that is estimated by this approach and that uses peak profiling at a single flow rate will be represented by the term "$k_{d,s}$" throughout the remainder of this current report.

Peak Profiling at Multiple Flow Rates

It is possible to rearrange eq 3 into the following form and to use data from multiple flow rates to determine k_d (see Supporting Information for derivation).

$$H_R - H_M = \frac{2 \cdot u \cdot k}{k_d \cdot 1 + k^2} = H_k \quad (8)$$

It is interesting to note that the difference ($H_R - H_M$) in eq 8 is simply equal to the plate height contribution due to stationary phase mass transfer (H_k). Eq 8 can also be derived by using other methods when the same assumption is made.[53,60,61] This equation shows the link between peak profiling and the plate height method, in that peak profiling can now be seen to be a special subset of the latter. In addition, this equation demonstrates that peak profiling at a single flow rate, as represented by eq 3, assumes that H_M and H_R only differ in terms of their value for H_k, which contributes to H_R but not H_M. This assumption does not require that H_M is constant (e.g., this term would be expected to vary with flow rate according to the van Deemter equation or related expressions), but it does require that the value of H_M be the same under any given set of experimental conditions for both the retained and non-retained solutes that are being injected.

Eq 8 predicts that a plot of ($H_R - H_M$) versus the term ($u\ k$)/$(1+k)^2$ should result in a linear relationship with a slope equal to $2/k_d$. It will be shown later in this report how such a plot can be used to determine a dissociation rate constant for an analyte-ligand interaction based on data obtained at multiple flow rates, thereby increasing the accuracy and precision of the estimated k_d value. Dissociation rate constants that are determined through this multiple flow rate approach and by using a linear plot will be referred to in this discussion by using the term "$k_{d,l}$".

Effects due to Stagnant Mobile Phase Mass Transfer & Diffusion

It was indicated earlier that one simplifying assumption made in both eqs 3 and 8 is that the retained and nonretained species have all the same band-broadening contributions to their total measured plate height except for the contribution due to stationary phase mass transfer (H_k). However, the plate height contribution due to stagnant mobile phase mass transfer for a retained and a non-retained species may not be identical for these two solutes due the dependence of this band-broadening process on the retention factor k.[50] It is possible to account for this effect in the use of multiple flow rates for peak profiling method by expanding eq 8 into the form shown in eq 9 (see derivation in Appendix).

$$H_R - H_M = \frac{u \cdot k}{1 + k^2} \cdot \left[\frac{2}{k_d} + \frac{d_p^2 2 + 3 \cdot k}{60 \cdot \gamma \cdot D} \right] \quad (9)$$

In this equation, γ is the tortuosity factor, D is the diffusion coefficient for the analyte or non-retained solute in the bulk mobile phase, and d_p is the particle diameter of the support material. Eq 9 is similar in form to eq 8 in that it predicts that a linear relationship will exist between ($H_R - H_M$) and ($u\ k$)/$(1+k)^2$; however, the slope of this plot now depends on two general terms, as given in eq 10. The first of these two terms ($2/k_d$) represents the contribution to the slope due to stationary phase mass transfer. The second term represents the contribution to the slope due to stagnant mobile phase mass transfer.

$$m = \left[\frac{2}{k_d} + \frac{d_p^2 \, 2+3 \cdot k}{60 \cdot \gamma \cdot D} \right] \quad (10)$$

Eq 10 predicts that the contribution from stagnant mobile phase mass transfer will cause the measured slope m to vary with the particle diameter (d_p) of the support material in the column. This observation makes it possible to correct for the effect of stagnant mobile phase mass transfer on this measured slope by performing peak profiling on multiple columns that contain packing materials with different but known particle sizes. If the slope from eq 9 is determined for several such columns, a plot of this slope can be made versus d_p^2, which is predicted by eq 10 to give an intercept that provides the true value for the dissociation rate constant, k_d. An alternative approach that can be used when comparing columns with significantly different activities and values for *k* is to plot the slope m versus the term d_p^2 (2+3 *k*), which also gives an intercept that can be used to obtain k_d.

It should be noted at this point that the derivation of eq 10 does assume that the ratio of the void volume and pore volume in the column is approximately equal to two (i.e., V_M/V_P = 2), which is a typical value for porous silica particles[50] and for the specific materials employed in this study (note: this value is also essentially the same for porous silica with different particle sizes, as used in this report). However, if this is not the correct value for this ratio, it will affect only the slope that is obtained for a plot of m versus d_p^2 and not the intercept. As a result, changes in the value of this ratio will not affect the final value for k_d that is obtained.

EXPERIMENTAL

Reagents

The L-tryptophan (>99.5% pure) was obtained from Fluka (Seelze, Germany) and the HSA (essentially fatty acid free, >96%) was from Sigma (St. Louis, MO). The Nucleosil Si-300 (5, 7 or 10 μm particle diameter, 300 Å pore size) was from Machery-Nagel (Duren, Germany). Reagents for the bicinchoninic acid (BCA) protein assay were from Pierce (Rockford, IL). All other chemicals were reagent-grade or better. All aqueous solutions were prepared with water obtained from a Nanopure water system (Barnstead, Dubuque, IA).

Apparatus

The chromatographic system consisted of a SPD-10AV UV/Vis detector and a LC-10AD pump controlled by an SCL-10A system controller from Shimadzu (Columbia, MD). Samples were injected using a SpectraSystem AS3000 Autosampler (Thermoseparations, Waltham, MA) equipped with a 5 μl sample loop. The columns were maintained at a constant temperature of 37.0 (± 0.1)°C using a water jacket from Alltech (Deerfield, IL) and a Fisher Scientific 9100 circulating water bath (Westbury, NY). Chromatograms were acquired using programs written in LabView 5.0 (National Instruments, Austin, TX). The statistical moments of the chromatographic peaks were determined using PeakFit 4.12 (Systat Software, San Jose, CA), in which moment analysis was performed using an EMG fit with a linear progressive baseline. The residual option in PeakFit was used to determine the best fit for the chromatographic peaks.

Column Preparation

Three sets of columns (each set containing one immobilized HSA column and one control column) were prepared using the 5, 7, or 10 μm particle size silica. To make these columns, the silica was first converted to a diol form.[62] The diol content of these supports was

determined in triplicate to be 300 (± 50), 231 (± 16), and 280 (± 19) μmol diol (± 1 S.D.) per gram of silica, respectively, as measured using an iodometric capillary electrophoresis assay.[63] Each type of silica was then split into two portions, with one portion being used to immobilize HSA and the other portion being taken through all of the same reaction steps but with no HSA being added during the immobilization step. The immobilized HSA support and corresponding control support were both prepared by the Schiff base method, as described previously.[7]

The protein content of each HSA support was determined in triplicate by a BCA protein assay,[64] using HSA as the standard and the control support as the blank. The measured protein content was 68 (± 4), 57 (± 3), and 63 (± 4) mg HSA per gram of silica for the 5, 7, and 10 μm HSA silica supports; the effective concentration of HSA (i.e., moles protein/void volume) in the columns prepared with these supports were 540 (± 30), 450 (± 20), and 500 (± 30) μM, respectively. Each type of HSA support or control support was downward slurry-packed at 24 MPa (3500 psi) into a separate stainless steel column (5 cm × 4.6 mm i.d.) using pH 7.4, 0.067 M potassium phosphate buffer as the packing solution All columns were stored at 4°C in pH 7.4, 0.067 M potassium phosphate buffer when not in use.

Chromatographic Experiments

All chromatographic studies were carried out at 37.0°C and in pH 7.4, 0.067 M potassium phosphate buffer as the mobile phase in order to mimic physiological conditions. All samples containing L-tryptophan or sodium nitrate (used as a non-retained solute) were prepared in this mobile phase (note: injections of 25 μM L-tryptophan on the control column were also explored for use in measurements of H_M). The solutions of L-tryptophan were prepared fresh each day to avoid any effects due to the slow degradation of this analyte in an aqueous solution.[65–67]

The elution of L-tryptophan was monitored at 220 nm and the elution of sodium nitrate was monitored at 205 nm. All experiments were performed within five months of column preparation and each column was used for less than 150 injections. Injections of 25 μM L-tryptophan and 25 μM sodium nitrate were made at 1 mL/min at regular intervals over the course of these experiments to monitor the activity and efficiency of the columns. This procedure was used to ensure the column had a consistent binding activity (as monitored by measuring k) and that the efficiency of the column did not change over time (as determined by monitoring the peak variances and plate heights). The second of these two measurements also helped to ensure that settling of the packing material or loss of support to form a small void space in the column had not occurred, a phenomenon which was found in preliminary studies to significantly increase H_M and lead to an overestimation of k_d or, in extreme cases, even negative k_d values The retention factors for L-tryptophan displayed a relative change between 2.2 to 12.6% for the various columns, indicating that the immobilized HSA had no appreciable changes in its binding to L-tryptophan during the course of these experiments. The measured plate heights for L-tryptophan, as determined from the same injections, changed by 0.4 to 2.3% over the given time period, while the plate heights measured for sodium nitrate changed by 9.6 to 13.8%. These latter results indicated that the efficiency of the columns were also consistent over the course of these experiments.

Injections were made in triplicate on the HSA or control column under each set of tested conditions. Identical injections were also made using a zero volume spacer/union in place of the column to correct for any additional elution times or band-broadening that was created by extra-column components of the chromatographic system. The analyte solutions that were used to examine the effect of sample concentration during the initial linear elution studies ranged from 5 to 250 μM for both L-tryptophan and sodium nitrate, which were injected at 1 mL/min to represent typical measurements of H_R or H_M, respectively. Most of

the later experiments used samples that contained 25 μM L-tryptophan or 25 μM sodium nitrate that were injected at flow rates of 1 to 3.5 mL/min. This entire range of flow rates was used to determine dissociation rate constants by using multiple flow rates and peak profiling method. The results obtained at 3.5 mL/min were used for comparison with the single flow rate approach that has been used in previous studies.[11]

Sample concentration effects in the single flow rate approach were examined by injecting 15 to 100 μM L-tryptophan or sodium nitrate onto the 7 μm particle size HSA column at 3.5 mL/min. Sample concentration effects in the multiple flow rate peak profiling method were studied using injections of 40 μM L-tryptophan on the 7 μm particle size HSA column at flow rates ranging from 1 to 3.5 mL/min. In all of these studies, a sample containing 25 μM sodium nitrate injected onto the same HSA column and was used as a non-retained void marker. Sample concentration effects were also studied on the 5 μm particle size HSA column.

RESULTS AND DISCUSSION

Selection of Analyte & Conditions for Peak Profiling at a Single Flow Rate

L-Tryptophan was employed throughout this study as a model solute to test and compare various methods for dissociation rate constant measurements. This solute is known to bind specifically to HSA at the indole-benzodiazepine site, or Sudlow site II,[14] and is commonly used in competition studies to determine if other solutes or drugs also bind to at this site.[1, 2, 6] The rate constants and equilibrium constants for this interaction have been previously characterized at various pH values and temperatures by using equilibrium dialysis[8] and affinity chromatography.[11,51,68,69] Under the conditions used in this study (pH 7.4 and 37°C), an association equilibrium constant of 1.1×10^4 M^{-1} has been reported for the binding of L-tryptophan with HSA;[3] and the dissociation rate constant has been estimated to be 3–6 s^{-1}, with the latter being determined by the plate height method and peak profiling at a single flow rate[11, 51] (i.e., the two approaches used as reference methods in this current report). All of these features made the L-tryptophan/HSA system a valuable tool for evaluation of the approaches described in this report for measuring drug-protein dissociation rates by HPAC.

The conditions used in this report with peak profiling method at a single flow rate were chosen to allow a direct comparison to be made with results reported in Ref. 11 for the L-tryptophan/HSA system. These conditions involved the use of a 5 cm × 4.6 mm i.d. HSA column containing silica particles with a pore size of 300 Å and an average diameter of 7 μm, with this column being operated at flow rates up to 3.5 mL/min. Additional studies were conducted to examine the effects of varying the support's particle diameter and the flow rate on the results obtained with peak profiling at a single flow rate. This work was initially carried out with a sample containing 25 μm L-tryptophan to provide linear elution behavior as well as a sufficient peak size for reliable retention time and variance measurements. However, the effect of working at other sample concentrations (e.g, the 100 μm L-tryptophan samples used in Ref. 11) was also considered (see next section).

Experiments performed early in this report examined the effect flow rate had on the measured variances and plate heights for L-tryptophan on HSA columns. Figure 3(a) shows typical plots of plate height versus linear velocity that were obtained for L-tryptophan and sodium nitrate (i.e., a non-retained solute) on an HSA column containing a 300 Å pore size, 7 μm particle size support. The linear velocities in this plot are equivalent to flow rates of 1.0 to 3.5 mL/min on the given column. The resulting plate height curves shown in Figure 3(a) agree with observations made in past band-broadening studies for L-tryptophan on similar HSA columns.[51,70] It was determined from these curves that the linear velocities

used in this study were at or above the minimum plate height in this van Deemter-type plot, as occurred at about 0.1 to 0.15 cm/s. Past work with the peak profiling method at a single flow rate sought to use high flow rates for dissociation rate constant measurements to reduce the effects of "non-kinetic" contributions in these experiments.[11] It can be seen from Figure 3(a) that the use of a lower flow rate in this approach would suffer from both a loss of accuracy (as other contributions to band-broadening become more important) and from a decrease in precision (as smaller differences occur between the band-broadening observed for the retained versus non-retained species. Thus, the selection of a suitably fast flow and linear velocity is critical in this particular technique.

Use of Peak Profiling at a Single Flow Rate

The data in Figure 3 were first examined by using eq 3 and peak profiling method at a single flow rate. It has been suggested previously by others that such a measurement should be made when the term η^2 is greater than one, as calculated by using eq 4 or 5. Such a situation occurred in Figure 3(a) when the linear velocity was greater than approximately 0.15. It has also been stated previously that accurate values for k_d in this method can only be determined when using a flow rate that is sufficiently high to cause the term κ (as given by eq 6 or 7) to approach a constant value.[11] In this particular study the value of κ was found to increase with linear velocity but did not reach a constant value over the range of flow rates that were tested, including the upper flow rate limit of 3.5 mL/min, as illustrated in Figure 3(b).

Figure 3(c) shows how the apparent dissociation rate constant measured by peak profiling at a single flow rate ($k_{d,s}$) changed with linear velocity for L-tryptophan injected onto the given HSA column. The data obtained at the three highest linear velocities in this plot (corresponding to flow rates of 2.5, 3 and 3.5 mL/min) gave $k_{d,s}$ values of 6.4 (± 0.1), 4.0 (± 0.2), and 3.1 (± 0.1) s^{-1}, respectively. Although these $k_{d,s}$ approached a limiting value at high linear velocities, there were significant differences between the estimated dissociation rate constants even the highest linear velocities tested in Figure 3(c). Using a lower linear velocity resulted in an increase in $k_{d,s}$ as the value of H_R grew closer to H_M. At the lowest linear velocity that was sampled, the measured value for H_R was even slightly less than H_M (although statistically equivalent), which created an apparent value for $k_{d,s}$ that was negative. These observations all confirmed the need to use high linear velocities to obtain reasonable and consistent values for dissociation rate constants when using peak profiling at a single flow rate.

It is interesting that although the dissociation rate constants in Figure 3 and Ref. 11 were obtained using the same method, type of analyte, protein, column dimensions, support particle diameter, and mobile phase, there were notable differences in the final results. The best agreement was obtained between the $k_{d,s}$ value of 6.4 (± 0.1) determined in Figure 3 at 2.5 mL/min and the "kinetic limited" value of 6.9 (± 0.03) reported in Ref. 11 at 3.5 mL/min. In addition, the $k_{d,s}$ found in this current study for L-tryptophan and HSA appeared to approach a value below 3 s^{-1} as the flow rate was increased to 3.5 mL/min. These differences may be due to the use of different immobilization methods, protein contents or packing efficiencies for the HSA supports used in these two studies. For example, the column in Ref. 11 had an effective concentration for active immobilized HSA of 181 μm, while the HSA columns in this current study had total concentrations between 450 to 540 μm and active concentrations were conservatively estimated to be in range of 225 to 300 μm.[7] Regardless of the cause of the difference, these results do indicate that column-to-column variability can affect the optimum flow rate conditions and apparent dissociation rate constants that are obtained when using peak profiling at a single flow rate. If this factor is not considered, it can result in a systematic error in the final value of $k_{d,s}$ if a sufficiently high flow rate is not selected for such a measurement. This effect represents another limitation of using only a single flow rate in the peak profiling method.

The effect of the support material in the single flow rate, peak profiling method was examined more closely by preparing HSA columns that contained silica with particle sizes of 5, 7 or 10 μm particles and a pore size of 300 Å. These supports were all prepared by the same immobilization technique and had similar protein content (see Materials and Methods). However, the efficiency of these columns was different because they contained different diameter particles, a factor that affects stagnant mobile phase mass transfer and mobile phase mass transfer/eddy diffusion. HSA columns containing these supports gave the same general behavior for plate height curves and plots of κ versus linear velocity as shown in Figure 3 for HSA columns containing 7 μm silica particles. However, the apparent dissociation rate constants measured with these columns did differ when the same flow rate was used for these studies. Table 1 shows the results obtained when working at a flow rate of 3.5 mL/min (i.e., the highest flow rate used in Figure 3). The smallest diameter and most efficient support (5 μm particle size) gave the largest estimate of the dissociation rate constant (4.1 s^{-1}), with a two-fold decrease in $k_{d,s}$ being found as the particle size was increased to 10 μm.

This last set of results indicated that the efficiency and diameter of the support material can have a significant effect on the apparent dissociation rate constant that is measured when using peak profiling at a single flow rate. The change seen in $k_{d,s}$ with particle size also indicates that the difference between the plate height of the retained and non-retained species in this approach is not necessarily equal to only the plate height contribution due to stationary phase mass transfer, as is assumed in eqs 3 and 8. Instead, these results suggest that this difference also reflects contributions due to other band-broadening processes that are affected by the particle diameter of the support, such as the stagnant mobile phase mass transfer and mobile phase mass transfer/eddy diffusion.

The sample concentration dependence of peak profiling at a single flow rate was also assessed. This was examined by injecting at 3.5 mL/min various concentrations of sodium nitrate and L-tryptophan on an HSA column containing 7 μm diameter silica particles. It was found that H_M remained approximately constant once a sufficiently high concentration of sodium nitrate was injected (e.g., 25 μM), which allowed peaks for this solute to be of a sufficient size for accurate determination of its statistical moments. The value of H_R, however, showed a continual increase as the sample concentration of L-tryptophan was raised, indicating that some non-linear elution effects were present. The result was a slight decrease in $k_{d,s}$ with an increasing sample concentration of L-tryptophan, as shown in Figure 4 (Note: these studies were all conducted using 25 μM sodium nitrate as the non-retained solute). The value of $k_{d,s}$ changed from 3.6 (± 0.7) to 2.74 (± 0.03) s^{-1} at 3.5 mL/min when going from sample concentrations that ranged from 10 to 100 μM L-tryptophan (i.e., samples representing 0.011 to 0.11% of the estimated HSA column loading capacity), with the latter concentration being the value used in Ref. 11. The value of $k_{d,s}$ measured for 25 μM L-tryptophan (i.e., 0.03% of the HSA column loading capacity and the sample used throughout most of this current study) was 3.2 (± 0.2) s^{-1} at 3.5 mL/min. These results indicated that there can be a concentration dependence for $k_{d,s}$ when using peak profiling at a single flow rate. However, the effect in this case was relatively small compared to the changes noted in $k_{d,s}$ when varying the flow rate or particle diameter.

Selection of Conditions for Peak Profiling at Multiple Flow Rates

The limitations noted in the last section for peak profiling at a single flow rate indicated that an alternative and more robust technique was needed for dissociation rate constant measurements. An alternative technique that could be used over a broader range of flow rates is the plate height method. However, this approach can also present difficulties if there are only small changes in the band-broadening of the non-retained species as a function of flow rate. This problem can be illustrated with the plate height data for sodium nitrate in

Figure 3(a), for which a quite small slope was obtained. This small slope results in a large uncertainty in the final estimate of H_{sm} and in the final determined value of k_d. In some cases, the slope of the plate height curve for the nonretained species may even have a slightly negative value but one that is statistically equivalent to zero; this results in an apparent negative value of k_d if error propagation is not correctly considered. Both of these effects indicate the need for a more direct measure of k_d, as was considered in this report through the use of peak profiling at multiple flow rates.

Peak profiling at multiple flow rates, which can be viewed as an extension and modified version of the plate height method, was conducted in this study by using the same columns and support particles as used for peak profiling at a single flow rate in the previous section. The entire flow rate range considered in the single flow rate approach was also used for this work (i.e., 1.0 to 3.5 mL/min). As shown by the plate height curves to the left in Figure 5, this flow rate range extended from the minimum region of the plate height plots (i.e., where H_R and H_M had approximately the same value) to the linear region of these plots (where H_R became much greater than H_M). In addition, the upper flow rate of 3.5 mL/min made it possible to compare the methods examined in this study with those used in a previous report[11] while still providing a reasonable back pressure for these experiments (e.g., 7.0 MPa or 1030 psi at 3.5 mL/min on the HSA column containing 5 μm support particles).

The effect of varying the sample concentration of the analyte was again considered. In this case it was desired to not only have linear elution conditions but also to obtain consistent, positive values for $(H_R - H_M)$. An example of such an experiment is shown in Figure 6 for injections of various concentrations of L-tryptophan at 1 mL/min onto an HSA column containing 5 μm support particles; a fixed concentration of 25 μM was used for sodium nitrate as the non-retained solute, as found to be optimum in the previous section. This specific column was chosen for this study since it had the smallest diameter support and was the most efficient of the three columns used in this work. This column would be expected to give the smallest difference in plate height between the retained and non-retained species, making it easier to see any variations in $(H_R - H_M)$ due to a change in sample concentration. In addition, the flow rate of 1 mL/min was at or near the minimum region of the plate height plots, also creating a situation in which any variations in $(H_R - H_M)$ would be easier to detect and monitor.

The results in Figure 6 indicate that the value of $(H_R - H_M)$ increased as the concentration of L-tryptophan was raised. Concentrations up to 25 μM L-tryptophan gave $(H_R - H_M)$ values that agreed within ± 1 S.D. However, larger sample concentrations gave large increases in $(H_R - H_M)$ and lead to significant deviations from the results obtained when using L-tryptophan concentrations at or below 25 μM. Based on these results, a sample concentration of 25 μM L-tryptophan was used in all later peak profiling experiments. The effect of using higher sample concentrations on the apparent dissociation rate constant that is measured by using peak profiling at multiple flow rates will be examined in the next section.

General Results for Peak Profiling at Multiple Flow Rates

The use of eq 8 for conducting peak profiling at multiple flow rates was next considered. This work was carried out using the same data, samples and columns as employed in the previous work with peak profiling method at a single flow rate (i.e., 25 μM L-tryptophan or 25 μM sodium nitrate and flow rates that ranged from 1.0 to 3.5 mL/min). The right hand side of Figure 5 shows the resulting plots of $(H_R - H_M)$ versus $(u\ k)/(1+k)^2$ that were obtained for HSA columns that were prepared with support particles that were 5, 7 or 10 μm in diameter.

Good agreement with a linear response was generally observed for the plots of ($H_R - H_M$) versus (u k)/(1+k)^2. Correlations of 0.966 to 0.983 (n = 7) were obtained for these plots over the entire flow rate range that was studied. This response was in agreement with the linear behavior that was predicted for such a plot by eq 8. The slopes of these plots were then used along with eq 8 to estimate the dissociation rate constant for the L-tryptophan/HSA interaction on each of the columns. The rate constants that were obtained are listed in Table 1. The three types of supports that were tested gave slightly different values for the apparent dissociation rate constant (ranging from 1.5 to 2.2 s^{-1}). These differences were later found to be a result of the different particle sizes of the supports in these columns and the resulting differences in stagnant mobile phase mass transfer, as will be discussed in the next section. However, it should also be noted that the difference in these values was much less than that found when using single linear velocities for peak profiling (1.9 to 4.1 s^{-1} at 3.5 mL/min), a method which was also subject to changes in stagnant mobile phase mass transfer. A lower degree of variability in dissociation rate constant measurements was expected when using multiple flow rates for peak profiling because such an approach would tend to average out variations that would be obtained when using individual flow rates or columns. In addition, the multiple flow rate method appears to correct for some retention-dependent contributions to peak profiling that are seen when using a single flow rate, as described below.

The change in the apparent dissociation rate constant ($k_{d,l}$) that was obtained when comparing the plots of ($H_R - H_M$) versus (u k)/(1+k)^2 in Figure 5 was a result of the slightly different slopes for these plots. This variation in the slope was caused by differences in the relative contribution of stagnant mobile phase mass transfer to the results for each type of support, as predicted by eq 9 and as discussed in the next section. However, there were some other changes in these plots that were related to the slight differences in retention for L-tryptophan on the individual HSA columns and which did not affect the measured slopes. These latter changes were produced by a small decrease in the retention factor in going from the HSA column with a 5 μm diameter support to the columns that contained 7 μm or 10 μm diameter supports (i.e., k = 13.8 (± 0.1), 12.95 (± 0.02), 12.38 (± 0.02) at 1 mL/min, respectively, with similar trends being seen at other flow rates). A lower value for k resulted in a larger value for (u k)/(1+k)^2, which caused a net shift to the right on the x-axis in a plot of ($H_R - H_M$) versus (u k)/(1+k)^2 when using columns that contained an increasing support particle diameter. This slight change in retention is also believed to have contributed to a small shift in the y-axis for plots of ($H_R - H_M$) versus (u k)/(1+k)^2 in Figure 5. Similar changes in ($H_R - H_M$) with retention have been noted in previous work with HSA columns.[45] This second effect is believed to be due to changes in the plate height due to mobile phase mass transfer (H_m) with a change in the retention factor,[45] a phenomenon that has been suggested by others in work with chromatographic theory.[71,72] This dependence would affect the values of H_R and H_M differently, thus creating a constant shift in the ($H_R - H_M$) values on the y-axis. This shift was most evident for the column containing the 10 μm support particles, as would be expected since the relative size of H_m is proportional to particle size.

Because these retention-based effects tended to produce a net shift for all data points that was constant for a given type of support, they did not affect the slopes measured for the plots ($H_R - H_M$) versus (u k)/(1+k)^2 or the dissociation rate constants that were determined from these slopes. However, this retention dependence and resulting shift would be expected to affect the results of peak profiling at a single flow rate, in which H_m is assumed to be negligible or constant for the non-retained versus retained solutes and no corrections are made for changes in k as a result of differing column activities. When using peak profiling at a single flow rate, a shift in the value of ($H_R - H_M$) and/or (u k)/(1+k)^2 due to a change in retention would have contributed to the greater variability of this latter approach when comparing data obtained with different columns. This same type of shift would also explain

the tendency of the single flow rate, peak profiling method to give larger apparent dissociation rate constants when compared to the use of multiple flow rates for peak profiling.

The effect of a small increase in sample concentration on the results when using multiple flow rates for peak profiling was next examined. In this case, the concentration of L-tryptophan was raised from 25 μM to 40 μM and injected the HSA column containing a 7 μm diameter support. The flow range that was tested was the same as that shown in Figure 5 and 25 μM sodium nitrate was again injected as the non-retained solute. The resulting graph of $(H_R - H_M)$ versus $(u\ k)/(1+k)^2$ (data not shown) had greater curvature than the corresponding plot in Figure 5(b) (which also had a small amount of curvature) and a lower correlation coefficient of 0.929 (n = 7) for the best-fit line. Although this increased curvature resulted in a less precise estimate of the dissociation rate constant when using the 40 μM L-tryptophan sample, the value of 2.0 (± 0.4) s^{-1} that was obtained was still statistically equivalent to that found for a 25 μM sample (see Table 1). These data indicated that the use of multiple flow rates for peak profiling can provide robust dissociation rate constant measurements that are insensitive to small variations in sample concentration.

Effect of Differences in Stagnant Mobile Phase Mass Transfer

Although the use of multiple flow rates was found to increase the precision and decrease the inter-column variation in estimates of dissociation rate constants, both this method and the single flow rate approach may still give an apparent value of k_d that is affected by stagnant mobile phase mass transfer. The size of this effect was examined in this report by looking at how the slope of a plot of $(H_R - H_M)$ versus $(u\ k)/(1+k)^2$ (used to determine the apparent k_d) changed when this slope is plotted as a function of d_p^2, where d_p is the particle diameter of the support. According to eq 10, this second type of plot should produce a linear relationship in which the intercept gives the true value for the dissociation rate constant between the analyte and immobilized ligand. Figure 7 shows the graph that was actually obtained for the various support diameters used in this report. Although only three support diameters were examined in this particular case, these conditions did span over a 4-fold range in values for d_p^2 and appeared to give good agreement with the linear trend predicted by eq 10 over this range.

The intercept of Figure 7 gave a dissociation rate constant of 2.7 (± 0.2) s^{-1} for the L-tryptophan system, which was now corrected for any contributions due to stagnant mobile phase mass transfer. This result fell within the range of 1.9 – 6.9 s^{-1} that was obtained earlier in this current study and in Ref. 11 for this dissociation rate constant when using peak profiling at a single flow rate. In addition, this result agreed with data obtained in previous band-broadening measurements, which gave estimated dissociation rate constants at pH 7.4 of 4 (± 1) s^{-1} at 25°C or 5.5 (± 1) s^{-1} at 37°C.[45, 68]

The same data as used in Figure 7 were examined by preparing a plot of the measured slope versus d_p^2 $(2+3\ k)$. According to eq 10, such a plot would again allow the dissociation rate constant to obtained from the intercept while also correcting for the small differences in retention that were noted earlier for L-tryptophan on the various HSA columns that were used in these studies. This new plot was again found to be linear, with a correlation coefficient of 0.994 (n = 3). The intercept of this plot provided a value for k_d of 2.8 (± 0.2) s^{-1}, which was within 1 S.D. of the value obtained from Figure 7. The similarity of these values indicated that the small changes in retention noted for the various HSA columns did not lead to any appreciable errors in the value of k_d given by Figure 7. This result was expected in this particular case because the four-fold increase for d_p^2 in Figure 7 was much larger than the maximum column-to-column variation of 10–11% in k that was measured for the specific HSA columns that were used to obtain this plot. However, if this approach is to

be used with a system that exhibits a larger change in *k* between columns, it would be preferable to use eq 10 along with a plot of the measured slope versus d_p^2 (2+3 *k*) instead of the slope versus d_p^2 to minimize the effects of these differences in retention.

Several interesting observations can be made when comparing the final estimated k_d of 2.7 s^{-1} with the individual values that were obtained when using single or multiple flow rates for peak profiling. For instance, it was found that using peak profiling at a single flow rate did give a useful preliminary estimate for k_d in this case, but with a relatively large amount of variability being seen in the results of this approach depending on the particular experimental conditions that were used for this measurement (e.g., flow rate, sample size, and type of column, as noted in this report). A much smaller degree of variability was noted when using peak profiling at multiple flow rates. However, as expected from eq 10, the final value found for k_d after correcting for stagnant mobile phase mass transfer was always higher than the apparent values that were obtained when using peak profiling at multiple flow rates if no correction was made for stagnant mobile phase mass transfer. The column with the smallest diameter support (5 μm particles, in this case), gave the closest estimate of k_d in multiple flow rate studies compared to the extrapolated value from Figure 7, with an error of only 18%. The other columns gave errors versus the extrapolated value for k_d of 26% and 44% for the 7 μm and 10 μm diameter supports, respectively, when using multiple flow rates with peak profiling. The use of affinity supports with even smaller diameters or smaller contributions to stagnant mobile phase mass transfer (e.g., non-porous or monolithic media)[74–76] would be expected to give even closer agreement in the apparent and actual values for k_d in such an experiment; such materials might be used in future work to minimize these errors and avoid the need for using multiple columns in these studies.

The fit of the data in Figure 7 was further examined by using the slope that was obtained for the best-fit response. According to eq 10, this slope is related to the retention factor for the solute (*k*, a known parameter) and the product γD, where γ is the tortuosity factor for the solute as it moves within the support particles and D is the solute's diffusion coefficient in the bulk mobile phase. If the tortuosity factor is assumed to be in the range of 0.1 to 0.5,[50] the resulting diffusion coefficient would be in the range of 12.0 (± 1) × 10^{-6} to 2.4 × 10^{-6} (± 0.2) cm^2/s, respectively. These diffusion coefficients are in a reasonable range for a small solute such as L-tryptophan [71] again indicating that there is good agreement between the response that is predicted by eq 10 and the experimental results noted in this study.

Effect of Changes in Stagnant Mobile Phase Mass Transfer

One assumption made in the derivation of both eqs 9 and 10 (as well as eqs 3 and 8) is that the rate of stagnant mobile phase mass transfer is the same for the non-retained species and the retained analyte. This assumption requires that the product $\gamma \cdot D$ in eqs 9 and 10 be the same for these two species. However, an expanded form of eq 10 can be obtained that does not make this assumption, as shown below in eq 11 (see Appendix).

$$m = \left[\frac{2}{k_d} + d_p^2\left(\frac{1+2\cdot k^2}{60\cdot \gamma\cdot D_R\cdot k} - \frac{1+k^2}{60\cdot \gamma\cdot D_M\cdot k}\right)\right] \quad (11)$$

This expanded equation uses two separate stagnant mobile phase mass transfer terms, as shown in parentheses to the right of eq 11. For the sake of simplicity, the difference in these two terms is represented by a difference in their diffusion coefficients for the retained and non-retained species, as represented by D_R and D_M, respectively. However, the above relationship could also be written in a form that allows both the tortuosity factor and diffusion coefficient to vary between the retained and non-retained species by using the combined terms $(\gamma \cdot D)_R$ and $(\gamma \cdot D)_M$ instead of $\gamma \cdot D_R$ and $\gamma \cdot D_M$ in eq 1.

According to eq 11, a plot of the measured slope m versus d_p^2 for a peak profiling study will again give a linear plot. The slope of this plot will be affected by a difference in stagnant mobile phase mass transfer between the retained and non-retained solute, but the intercept of this plot will still be equal to $2/k_d$. Thus, eq 11 indicates the approximation made in eq 10 that the rate of stagnant mobile phase mass transfer is the same for the retained and non-retained solutes will not affect the final value for k_d that is determined when using peak profiling at multiple flow rates and with multiple columns that have supports with different particle sizes.

It is possible, however, that a change in the rate of stagnant mobile phase mass transfer between the retained and non-retained species could lead to differences in dissociation rate constants that are estimated using individual columns. To determine the size of this effect, peak profiling studies on a single type of column were conducted using two independent measures of H_M: one set using sodium nitrate injected onto an HSA column (as used previously throughout this report), and second set using injections of L-tryptophan on an inert control column (i.e., based on injections of 25 μM L-tryptophan). These values were compared using data for the HSA and control columns that contained 7 μm support particles.

The results obtained when using sodium nitrate on the HSA column to measure H_M were given earlier in Figure 3. A similar plot was obtained over the same range of flow rates when using injections of L-tryptophan on the control column to estimate H_M (data not shown; correlation coefficient = 0.981, n = 7). The slope of this second plot gave an estimated value for $k_{d,l}$ of 1.7 (± 0.2) s^{-1}. This result was within one standard deviation of the $k_{d,l}$ value of 2.0 (± 0.2) that was obtained when using sodium nitrate as the non-retained species on the HSA column (see Table 1), with the two values differing by 15%. Thus, it was concluded that differences in the rate of stagnant mobile phase mass transfer for sodium nitrate versus L-tryptophan did not create any significant errors in the estimated dissociation rate constants measured in this study.

The result of this comparison is not surprising because L-tryptophan and sodium nitrate have a similar size and both species are small compared to the pores of the support. These properties should have given these solutes approximately the same diffusion coefficients in the mobile phase and allowed both species to travel relatively freely between the flowing mobile phase and stagnant mobile phase regions of the column. It should be noted, though, that deviations in eqs 9 and 10 (or eqs 3 and 8) due to difference in the rate of stagnant mobile phase mass transfer could become important if much larger solutes are being examined, making restricted diffusion in the pores more important, or if there are large differences in the sizes and diffusion coefficients of the non-retained and retained solutes. In this situation it would advisable to simply use the same species to measure both H_R and H_M through the use of an appropriate control column.

One possible issue when using separate protein and control columns to measure H_R and H_M is that small differences may be created in the apparent pore diameters and values of $\gamma \cdot D$ due to the presence and absence of the immobilized protein. The results obtained here when using sodium nitrate on an HSA column or L-tryptophan on a control column indicate that this issue was not a major concern for the dissociation rate constant measurements made in this study. In addition, the plate height values for L-tryptophan and sodium nitrate that were compared in all previous sections of this work were obtained by using only the HSA columns, which would have automatically corrected for such an effect.

CONCLUSIONS

This report examined the development of an improved, alternative method for measuring the rates of drug-protein dissociation by using HPAC and peak profiling. This approach used band-broadening measurements for both a retained analyte and a non-retained solute at several flow rates on an immobilized protein column to determine the dissociation rate constant for the analyte-protein interaction. Work with chromatographic theory was employed to derive equations that could be used with this approach on a single column, as well as with multiple columns to correct for the impact of stagnant mobile phase mass transfer. This approach was tested by using the interaction of L-tryptophan with HSA as a model, and was found to give good agreement with dissociation rate constants that were determined by reference methods.

The technique described in this report can be applied to other biological systems and should be valuable for the high-throughput determination of drug-protein dissociation rates. The use of multiple flow rates for peak profiling was found to give more robust, consistent results than when using peak profiling at a single flow rate, while also allowing peak profiling to conducted over a broader range of flow rate conditions.[11, 58] The use of multiple columns with different support diameters made it possible to correct for any differences in band-broadening due to stagnant mobile phase transfer for the non-retained versus retained solutes, as well as to examine the effects of these differences in such work. The results obtained by this approach were comparable to values provided by previous band-broadening studies;[51,73] however, the peak profiling approach was more convenient to use and provided estimates of k_d with fewer injections and in shorter periods of time. This approach also has several possible advantages over SPR in that it is not limited to a particular type of detection means and kinetics can be determined for a broader range of affinity systems.[35] The fact that only a small amount of analyte is required per injection is another attractive feature of this method. All of these properties should make this approach useful in the study of additional solute-ligand interactions and in the high-throughput screening of solute-protein interactions to identify or characterize new drug targets.

Supplementary Material

Refer to Web version on PubMed Central for supplementary material.

Acknowledgments

The authors would like to thank the Society of Analytical Chemists of Pittsburgh for their support of J. Schiel through an ACS Division of Analytical Chemistry Graduate Fellowship. This work was supported by the National Institutes of Health under grant R01 GM044931 and was performed in facilities renovated with support under grant RR015468-01.

NOMENCLATURE

A	Analyte
A-P	Analyte-protein complex (or analyte complex with a binding agent P)
D	Diffusion coefficient; D_M and D_R are the diffusion coefficients for non-retained and retained solutes, respectively.
$\mathbf{d_p}$	Support particle diameter
$\mathbf{t_M}$	Column void time (corrected for extra column time)
$\mathbf{t_R}$	Retention time for an analyte on a column (corrected for extra column time)

H	Total plate height
$\mathbf{H_k}$	Plate height contribution due to stationary phase mass transfer
$\mathbf{H_l}$	Plate height contribution due to longitudinal diffusion
$\mathbf{H_m}$	Plate height contribution due to mobile phase mass transfer and eddy diffusion
$\mathbf{H_M}$	Total plate height for a non-retained species
$\mathbf{H_R}$	Total plate height for a retained species
$\mathbf{H_{sm}}$	Plate height contribution due to stagnant mobile phase mass transfer
k	Retention factor
$\mathbf{k_{-1}}$	Mass transfer rate constant describing movement of a solute from the stagnant mobile phase to the flowing mobile phase in a column
$\mathbf{K_a}$	Association equilibrium constant
$\mathbf{k_a}$	Association rate constant
$\mathbf{k_d}$	Dissociation rate constant
$\mathbf{k_{d,l}}$	Dissociation rate constant, as determined using the multiple flow rate peak profiling method
$\mathbf{k_{d,\,s}}$	Dissociation rate constant, as determined using peak profiling at a single linear velocity
L	Column length
m	Slope of a linear plot to examine peak profiling data
n	Number of theoretical plates
P	Protein or binding agent
u	Linear velocity of the mobile phase
$\mathbf{V_M}$	Column void volume
$\mathbf{V_P}$	Pore volume
$\boldsymbol{\kappa}$	Kinetic factor for peak profiling, as defined by eq 7
$\boldsymbol{\gamma}$	Tortuosity factor
$\boldsymbol{\sigma_M}$	Standard deviation for the peak of a non-retained species (corrected for extra-column variance)
$\boldsymbol{\sigma_R}$	Standard deviation for the peak of a retained species (corrected for extra-column variance)
$\boldsymbol{\sigma_M^2}$	Peak variance for a non-retained species (corrected for extra-column variance)
$\boldsymbol{\sigma_R^2}$	Peak variance for a retained species (corrected for extra-column variance)

APPENDIX

The contributions to chromatographic efficiency are often assumed to be additive when described in terms of variance or plate height. The total plate height for a solute eluting from a column is typically represented as the sum of contributions due to eddy diffusion and mobile phase mass transfer (H_m), longitudinal diffusion (H_l), stagnant mobile phase mass transfer (H_{sm}), and stationary phase mass transfer (H_k),[45,50]

$$H_{total} = \frac{L \cdot \sigma_i^2}{t_i^2} = H_m + H_1 + H_{sm} + H_k \quad \text{(A1)}$$

where t_i and σ_i represent the elution time and standard deviation for the observed peak of solute i.

It was noted earlier that eq 3, as used in the past for peak profiling, assumes that the difference between the total measured plate heights for a retained and non-retained species will be equal to the plate height contribution due to stationary phase mass transfer, or ($H_R - H_M$) = H_k.[11,53,58] However, the plate height term H_{sm} is also known to depend on retention and, therefore, could be quite different in size for a retained versus non-retained species. If this is the case, the H_{sm} would be expected to also make up part of the difference noted in the values of H_R and H_M. A better representation of ($H_R - H_M$) that accounts for this difference is given in eq A2,

$$H_R - H_M = H_k + H_{sm,R} - H_{sm,M} \quad \text{(A2)}$$

where $H_{sm,R}$ and $H_{sm,M}$ are the plate height contributions due to stagnant mobile phase mass transfer for the retained and non-retained species, respectively.

The following general expression has been derived in previous studies to describe H_{sm},[60]

$$H_{sm} = \frac{2 \cdot u \cdot V_P \left(1 + \frac{V_M}{V_P} \cdot k\right)^2}{k_{-1} \cdot V_M \, 1 + k^2} \quad \text{(A3)}$$

in which k_{-1} is the mass transfer rate constant that describes the movement of a solute from the stagnant mobile phase to the flowing mobile phase region of the column. The value of H_{sm} that is obtained in this case can be used to represent $H_{sm,R}$ in eq A2 and in the case of a non-retained species (for which $k = 0$), eq A3 reduces to $H_{sm,M} = (2\ u\ V_P)/(k_{-1}\ V_M)$. Substituting eq A3 and the relationship for H_k that is given in eq 8 into eq A2 gives the following expanded relationship.

$$H_R - H_M = \frac{2 \cdot u \cdot k}{k_d \cdot 1 + k^2} + \frac{2 \cdot u \cdot V_P \left(1 + \frac{V_M}{V_P} \cdot k\right)^2}{k_{-1} \cdot V_M \, 1 + k^2} - \frac{2 \cdot u \cdot V_P}{k_{-1} \cdot V_M} \quad \text{(A4)}$$

Eq A4 can be simplified by factoring out ($2\ u\ V_P/k_{-1}\ V_M$) from the two terms on the far right-hand side of this relationship. It is assumed during this step that the mass transfer rate constant k_{-1} is approximately the same for the retained and non-retained species; this is a reasonably good assumption for low mass molecules that have similar diffusion coefficients.[60] Eq A4 can also be simplified for work with porous silica packing materials by using the fact that $V_M/V_P \approx 2$ for most of these supports.[50] Making both of these modifications to eq A4 produces eq A5 (Note: similar expressions can be obtained when using values for V_M/V_P other than two).

$$\text{If } V_M/V_P \approx 2 : H_R - H_M = \frac{2 \cdot u \cdot k}{k_d \cdot 1 + k^2} + \frac{u}{k_{-1}} \left[\frac{1 + 2 \cdot k^2}{1 + k^2} - 1\right] \quad \text{(A5)}$$

Using the expression in eq A5, the numerator and denominator in the term on the far right (representing the differences in H_{sm} for a retained versus non-retained species) can both be multiplied by $k/(1+k)^2$ to give eq A6.

$$H_R - H_M = \frac{2 \cdot u \cdot k}{k_d \cdot 1+k^2} + \frac{u}{k_{-1}} \left[\frac{1+2 \cdot k^2}{1+k^2} - 1 \right] \cdot \left[\frac{\frac{k}{1+k^2}}{\frac{k}{1+k^2}} \right] \quad \text{(A6)}$$

Cancellation of the common terms in eq A6 allows $(u\ k)/(1+k)^2$ to be factored out of this relationship, thus giving eq A7.

$$H_R - H_M = \frac{u \cdot k}{1+k^2} \left[\frac{2}{k_d} + \frac{2+3k}{k_{-1}} \right] \quad \text{(A7)}$$

This equation is now in a similar form to that shown for previously for eq 8 but no longer makes that assumption that H_{sm} is the same for both the retained and non-retained species.

The difference between the new expression in eq A7 and eq 8 is that the slope term on right has two contributing terms, one representing the contribution due to stationary phase mass transfer and other accounting for the dependence of the stagnant mobile phase mass transfer term on retention. The slope term of the expanded relationship in eq A7 is given by eq A8.

$$m = \left[\frac{2}{k_d} + \frac{2+3k}{k_{-1}} \right] \quad \text{(A8)}$$

This expression shows that it is possible to distinguish between the two sources of band-broadening that contribute to this slope by relating the second term of eq A8 to the particle diameter of the support. This can be accomplished by substituting into this equation the relationship $k_{-1} = 60\ \gamma\ D/d_p^2$, which results in eq 10.

An assumption made in the derivation of eqs 9 and 10 (as well as eqs 3 and 8) is that the rate of stagnant mobile phase mass transfer is the same for the retained and non-retained species. A similar derivation to that used to obtain eq A7 can be used to determine the effect of this assumption. Such a derivation starts with a modified form of eq A4 in which two different values for k_{-1} are used for the retained and non-retained species (i.e., $k_{-1,R}$ and $k_{-1,M}$, respectively. Because $k_{-1,R}$ and $k_{-1,M}$ are no longer assumed to be identical in value, as is done in the derivation of eq 10, the only common term that can be factored out of this modified version of eq A4 is now $(2\ u\ V_P/V_M)$. The remainder of the derivation is the same as given earlier for eq 10. During this process, a substitution is made using the fact that $k_{-1,R} = (60\ \gamma\ D_R/d_p^2)$ and $k_{-1,M} = (60\ \gamma\ D_M/d_p^2)$ to give the final form shown in eq 11.

References

1. Bertuzzi A, Mingrone G, Gandolfi A, Greco AV, Ringoir S, Vanholder R. Clin. Chim. Acta. 1997; 265:183–192. [PubMed: 9385460]
2. Chen J, Ohnmacht C, Hage DS. J. Chromatogr. B. 2004; 809:137–145.
3. Hage DS. J. Chromatogr. B. 2002; 768:3–30.
4. Hethcote H, Delisi C. J. Chromatogr. 1982; 248:183–202.
5. Johansen K, Krogh M, Andresen AT, Christophersen AS, Lehne G, Rasmussen KE. J. Chromatogr. B. 1995; 669:281–288.
6. Kim HS, Hage DS. J. Chromatogr. B. 2005; 816:57–66.
7. Loun B, Hage DS. Anal. Chem. 1994; 66:3814–3822. [PubMed: 7802261]
8. McMenamy RH, Seder RH. J. Biol. Chem. 1963; 238:3241–3248. [PubMed: 14085368]

9. Miller TD, Pinderton TC. Anal. Chim. Acta. 1985; 170:295–300.
10. Schiel JE, Mallik R, Soman S, Joseph KS, Hage DS. J. Sep. Sci. 2006; 29:719–737. [PubMed: 16830485]
11. Talbert AM, Tranter GE, Holmes E, Francis PL. Anal. Chem. 2002; 74:446–452. [PubMed: 11811421]
12. Winzor, DJ.; Sawyer, WH. Quantitative Characterization of Ligand Binding. New York: Wiley-Liss; 1995.
13. Wang H, Zou H, Zhang Y. Anal. Chem. 1998; 70:373–377. [PubMed: 9450364]
14. Herve F, Urien S, Albengres E, Duche J-C, Tillement J-P. Clin. Pharmacokin. 1994; 26:44–58.
15. Peters, TJ. All About Albumin. Academic Press; 1995. **(We need to complete this reference)**
16. Berezhkovskiy LM. J. Pharm. Sci. 2006; 95:834–848. [PubMed: 16493592]
17. Smith, QR.; Fisher, C.; Allen, DD. Blood-Brain Barrier: Drug Delivery and Brain Pathology. Kobiler, D.; Lustig, S.; Shapira, S., editors. New York: Kluwer Academic/Plenum Publishers; 2000. p. 311-321.
18. Trainor GL. Expert Opin. Drug Discovery. 2007; 2:51–64.
19. Trainor GL. Annu. Rep. Med. Chem. 2007; 42:489–502.
20. Fenerty CA, Lindup E. J. Neurochem. 1989; 53:416–422. [PubMed: 2746229]
21. Lin TH, Lin JH. J. Pharmacol Exp. Ther. 1990; 253:45–50. [PubMed: 1970363]
22. Lin TH, Sawada Y, Sugiyama Y, Iga T, Hanano M. Chem. Pharmacol. Bull. 1987; 35:294–301.
23. Partridge, WM. Handbook of Physiology-Cellular Endocrinology. Conn, PM., editor. New York: Oxford University Press; 1998. p. 335-382.
24. Partridge WM, Landaw EM. J. Clin. Invest. 1984; 74:745–752. [PubMed: 6470138]
25. Partridge WM, Sakiyama R, Fierer G. J. Clin. Invest. 1983; 71:900–908. [PubMed: 6833493]
26. Riant P, Urien S, Albengres E, Renouard A, Tillement J-P. J. Neurochem. 1988; 51:1988.
27. Robinson PJ, Rapaport SI. Am. J. Physiol. 1986; 251:R1212–R1220. [PubMed: 3789202]
28. Videbaek C, Ott P, Paulson OB, Knudsen GM. J. Cereb. Blood Flow Metab. 1999; 19:948–955. [PubMed: 10478646]
29. Wang H, Wang Z, Lu M, Zou H. Anal. Chem. 2008; 80:2993–2999. [PubMed: 18355058]
30. Clarke W, Schiel JE, Moser A, Hage DS. Anal. Chem. 2005; 77:1859–1866. [PubMed: 15762597]
31. Ohnmacht CM, Schiel JE, Hage DS. Anal. Chem. 2006; 75:7547–7556. [PubMed: 17073425]
32. Buchholz L, Cai C-H, Andress L, Cleton A, Brodfuehrer J, Cohen L. Eur. J. Pharm. Sci. 2002; 15:209–215. [PubMed: 11849918]
33. Ohlson S. Drug Discovery Today. 2008; 13:433–439. [PubMed: 18468561]
34. Ohlson S, Shovari S, Fex T, Roland I. Anal. Biochem. 2006; 359:120–123. [PubMed: 17052679]
35. Rich RL, Day YSN, Morton TA, Myszka DG. Anal. Biochem. 2001; 296:197–207. [PubMed: 11554715]
36. Wan H, Bergstroem F. J. Liq. Chromatogr. Relat. Technol. 2007; 30:681–700.
37. Eccleston, JF. Spectrophotometry & Spectrofluorimetry. A Practical Approach. Harris, DA.; Bashford, CL., editors. Washington DC: IRL Press; 1987. p. 137-164.
38. Fitos I, Visy j, Kardos J. Chirality. 2002; 14:442–448. (There is a typo here in the names). [PubMed: 11984760]
39. Porter DJT. Biochem. Pharmacol. 1992; 44:1417–1429. [PubMed: 1417962]
40. Rietbrock N, LaBmann A. Naunyn-Schmiedeberg's Arch. Pharmacol. 1980; 313:269–274. [PubMed: 7432558]
41. Jozwiak K, Haginaka J, Moaddel R, Wainer I. Anal. Chem. 2002; 74:4618–4624. [PubMed: 12349962]
42. Jozwiak K, Hernandoz SC, Kellar KK, Wainer IW. J. Chromatogr. B. 2003; 797:373–379.
43. Jozwiak K, Ravichandran S, Collins JR, Moaddel R, Wainer IW. J. Med. Chem. 2007; 50:6279–6283. [PubMed: 17973360]
44. Jozwiak K, Ravichandran S, Collins JR, Wainer IW. J. Med. Chem. 2004; 47:4008–4021. [PubMed: 15267239]

45. Loun B, Hage DS. Anal. Chem. 1996; 68:1218–1225. [PubMed: 8651495]
46. Marszall MP, Moaddel R, Jozwiak K, Bernier M, Wainer IW. Anal. Biochem. 2008; 373:313–321. [PubMed: 18047824]
47. Moaddel R, Jozwiak K, Yamaguchi R, Wainer IW. Anal. Chem. 2005; 77:5421–5426. [PubMed: 16097790]
48. Moaddel R, Wainer IW. J. Pharm. Biomed. Anal. 2007; 43:399–406. [PubMed: 17095178]
49. Moore RM, Walters RR. J. Chromatogr. 1987; 384:91–103.
50. Walters, RR. Analytical Affinity Chromatography. Chaiken, IM., editor. Boca Raton: CRC Press; 1987. p. 117-156.
51. Yang J, Hage DS. J. Chromatogr. A. 1997; 766:15–25. [PubMed: 9134727]
52. Anderson DJ, Walters RR. J. Chromatogr. 1986; 376:69–85.
53. Muller AJ, Carr PW. J. Chromatogr. 1984; 284:33–51.
54. Wade JL, Bergold AF, Carr PW. Anal. Chem. 1987; 59:1286–1295.
55. Denizot FC, Delaage MA. Proc. Natl. Acad. Sci. U. S. A. 1975; 72:4840–4843. [PubMed: 1061072]
56. Pearlmutter AF, Dalton EJ. Biochemistry. 1980; 19:3550–3556. [PubMed: 7407058]
57. Swaisgood, HE.; Chaiken, IM. Analytical Affinity Chromatography. Chaiken, IM., editor. Boca Raton: CRC Press; 1987.
58. Swaisgood HE, Chaiken IM. Biochemistry. 1986; 25:4148–4155. [PubMed: 3741847]
59. Jeansonne MS, Foley JP. J. Chromatogr. Sci. 1991; 29:258–266.
60. Hage DS, Walters RR, Hethcote HW. Anal. Chem. 1986; 58:274–279. [PubMed: 3963388]
61. Horvath C, Lin H-J. J. Chromatogr. 1978; 149:43–70.
62. Larsson P-O. Methods Enzymol. 1984; 104:212–223. [PubMed: 6371445]
63. Chattopadhyay A, Hage DS. J. Chromatogr. A. 1997; 758:255–261. [PubMed: 9042737]
64. Smith PK, Krohn RI, Hermanson GT, Mallia AK, Gartner FH, Provenzano MD, Fujimoto EK, Goeke NM, Olson BJ, Klenk DC. Anal. Biochem. 1985; 150
65. Lee MG, Rogers CM. J. Parenteral Sci. Tech. 1988; 42:20–22.
66. Savige WE. Aust. J. Chem. 1971; 24:1285–1293.
67. Savige WE. Aust. J. Chem. 1975; 28:2275–2287.
68. Yang J, Hage DS. J. Chromatogr. 1993; 645:241–250. [PubMed: 8408417]
69. Yang J, Hage DS. J. Chromatogr. A. 1996; 752:273–285. [PubMed: 8900576]
70. Mallik R, Hage DS. J. Pharm. Biomed. Anal. 2008; 46:820–830. [PubMed: 17475436]
71. Karger, BL.; Snyder, LR.; Horvath, C. An Introduction to Separation Science. New York: Wiley; 1973.
72. Knox JH. J. Chromatogr. Sci. 1977; 15:352–364.
73. Yang, J. Ph.D. Thesis. Lincoln: University of Nebraska, Lincoln; 1995.
74. Mallik R, Hage DS. J. Sep. Sci. 2006; 29:1686–1704. [PubMed: 16970180]
75. Mallik R, Jiang T, Hage DS. Anal. Chem. 2004; 76:7013–7022. [PubMed: 15571354]
76. Gustavsson, P-E.; Larsson, P-O. Handbook of Affinity Chromatography. Hage, DS., editor. New York: Taylor and Francis; 2006. p. 15-34.

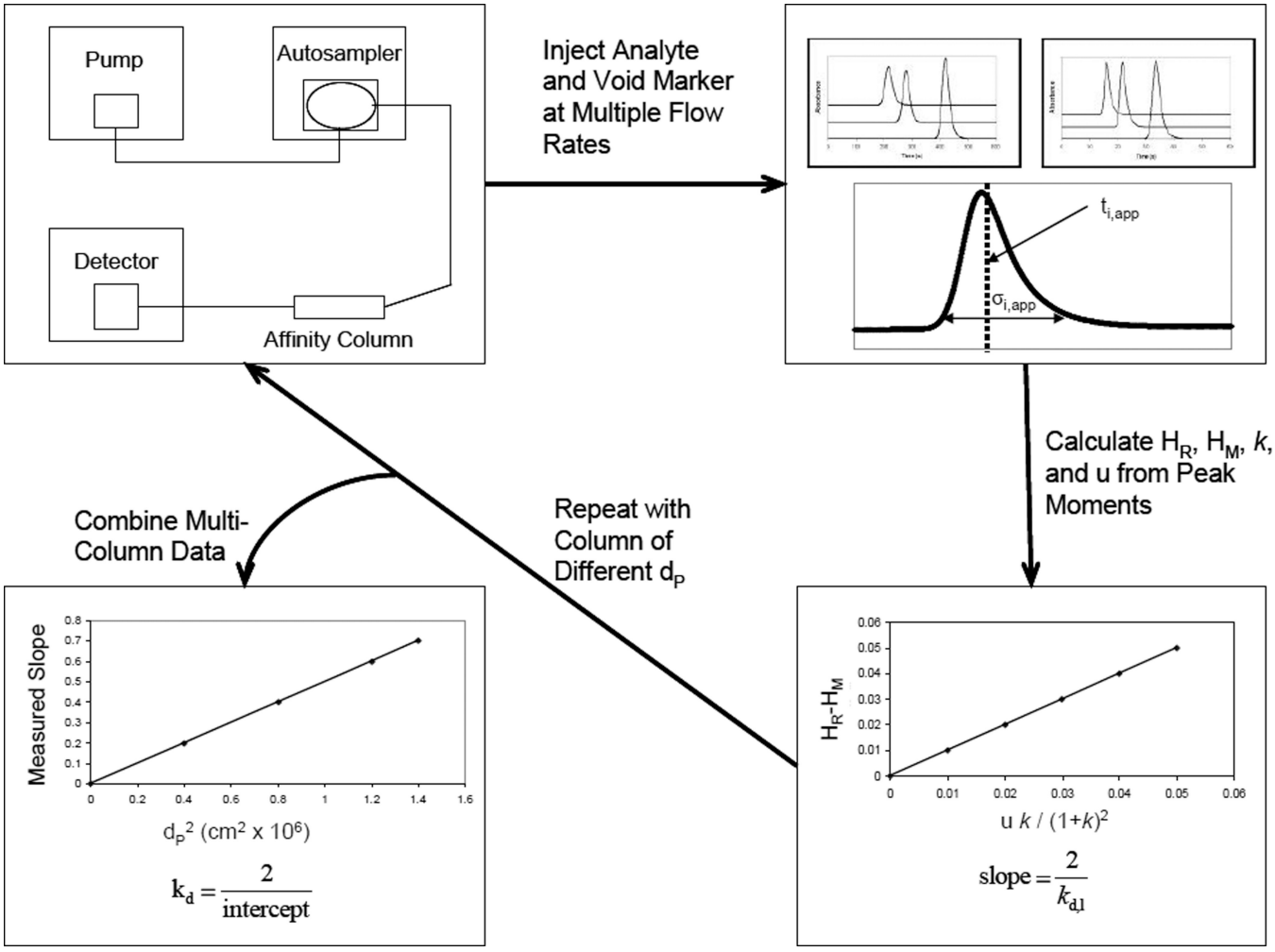

Figure 1.
Scheme for a peak profiling experiment. The various terms shown in this figure are defined and described in the text.

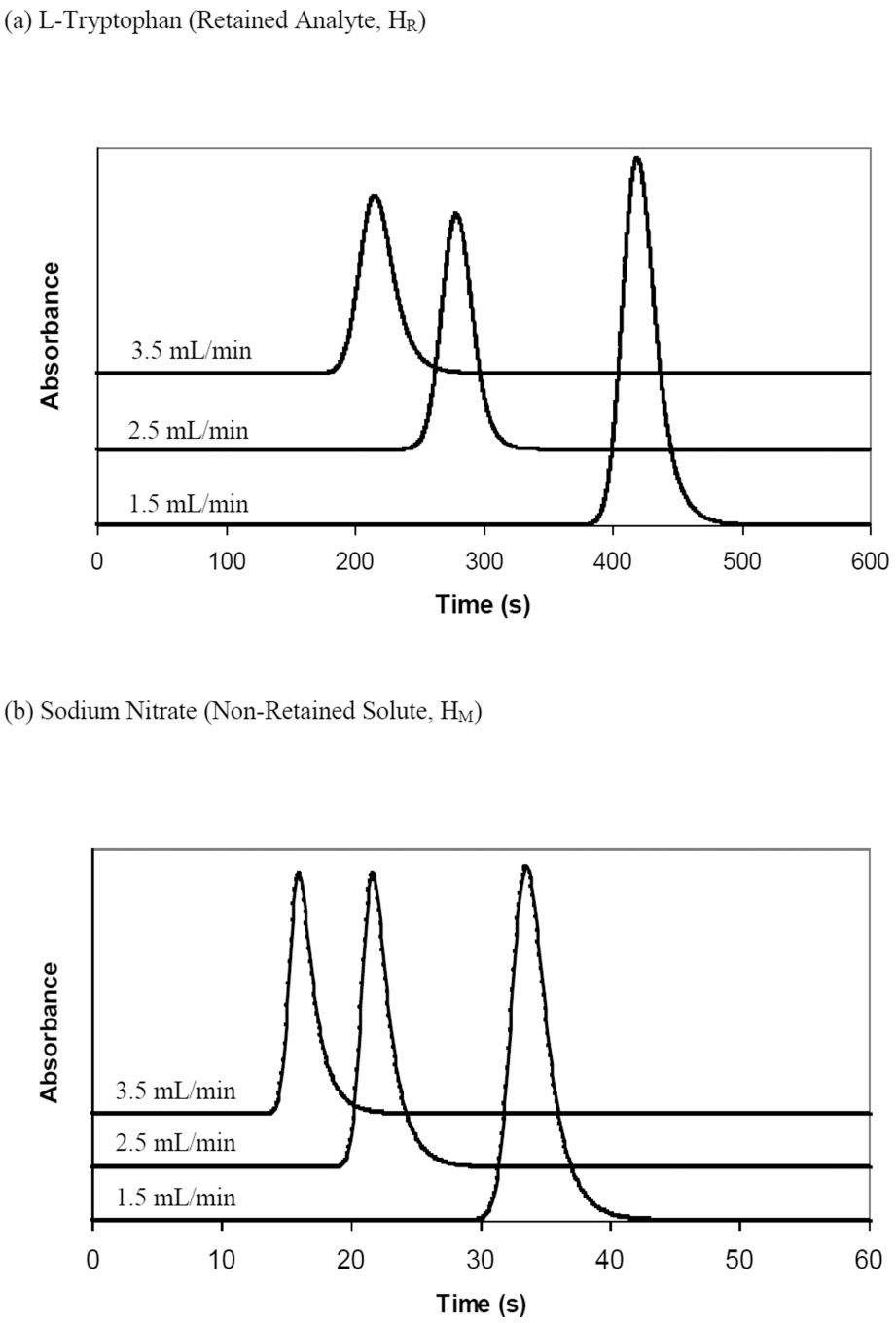

Figure 2.

Representative chromatograms for samples of (a) 25 μM L-tryptophan or (b) 25 μM sodium nitrate injected onto an HSA column that contained a support based on 300 Å pore size, 7 μm diameter silica. These samples were injected at the indicated flow rates and at 37°C using pH 7.4, 0.067 M potassium phosphate buffer as the mobile phase. Other conditions are given in the text.

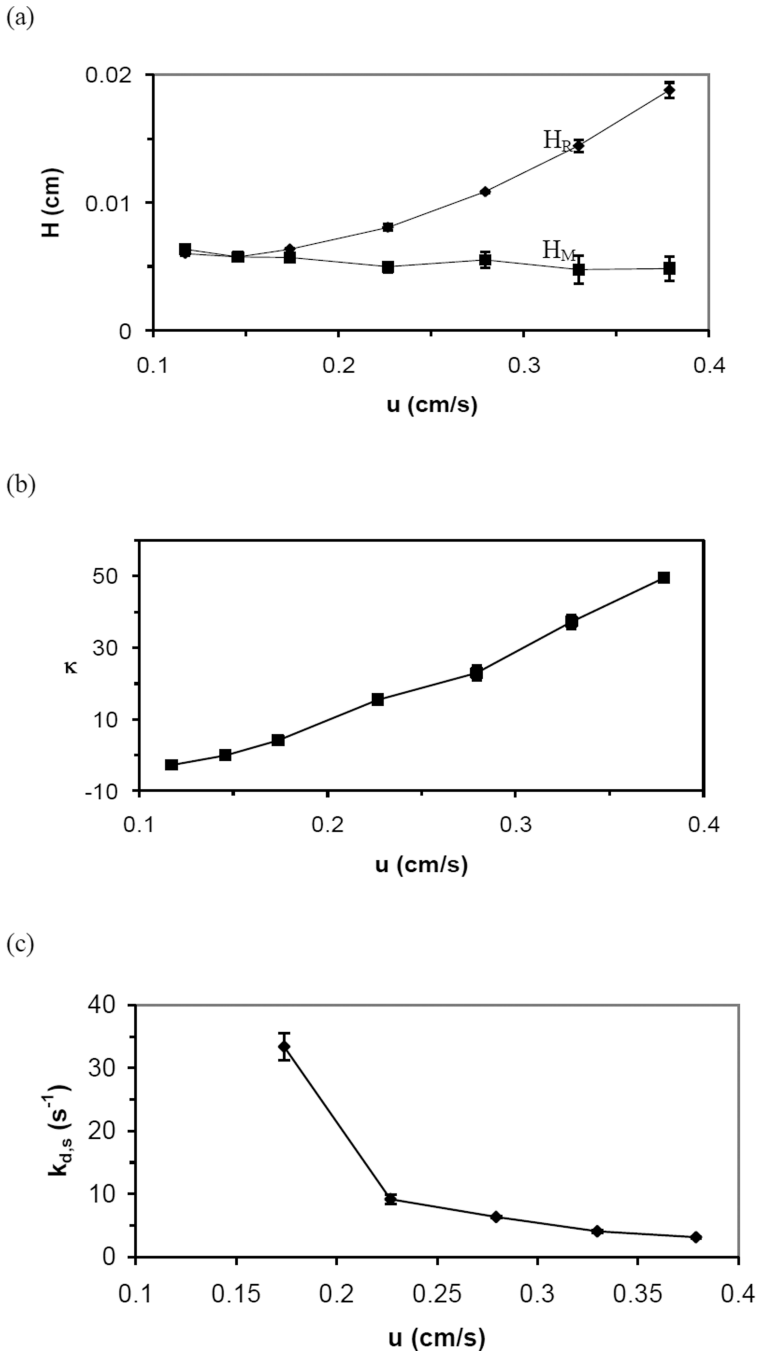

Figure 3.

Typical peak profiling results for injections of 25 μM L-tryptophan or 25 μM sodium nitrate onto an HSA column containing 7 μm diameter silica particles. The graphs in this figure show (a) plate height plots for L-tryptophan (H_R, ◆) and sodium nitrate (H_M, ■); (b) a plot of the kinetic factor κ versus linear velocity; and (c) a plot of the apparent value of $k_{d,s}$ for L-tryptophan, as calculated at various linear velocities by using peak profiling method at a single flow rate. The values for $k_{d,s}$ at the two lowest linear velocities in this study are not included in (c) because these values were either much larger the other values shown or had a negative value, as occurred in this case at the lowest flow rate, where the measured value of H_R was slightly less than H_M. The error bars represent a range of ± 1 S.D.

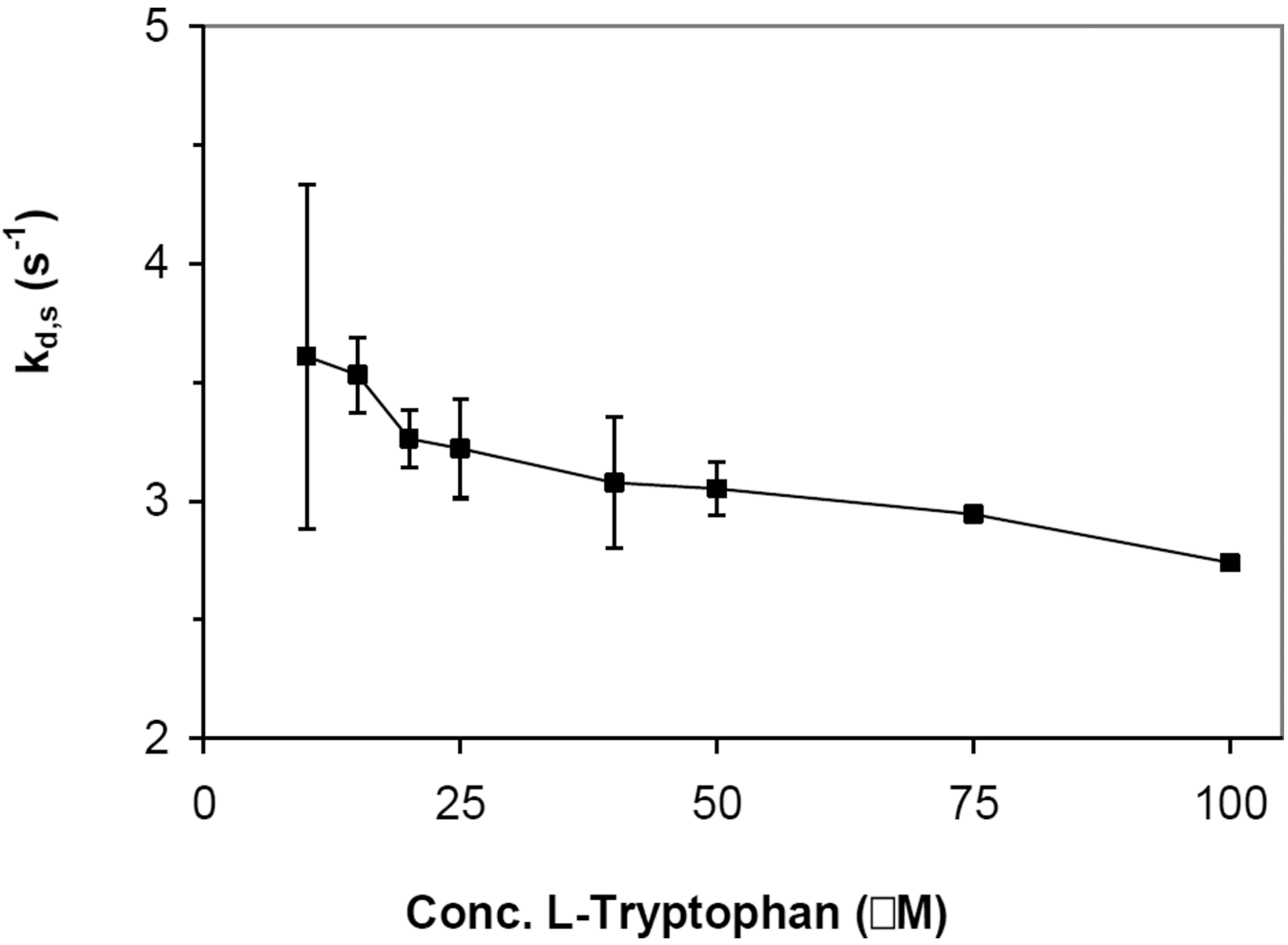

Figure 4.

Concentration dependence of $k_{d,s}$ determined for L-tryptophan using peak profiling at a single flow rate. Data presented is for injections of L-tryptophan concentrations ranging from 10 to 100 μM at a flow rate of 3.5 mL/min on the 7 μm HSA column. Void data for each calculation was for injections of 25 μM sodium nitrate under the same conditions. Error bars indicate ± 1 S.D.

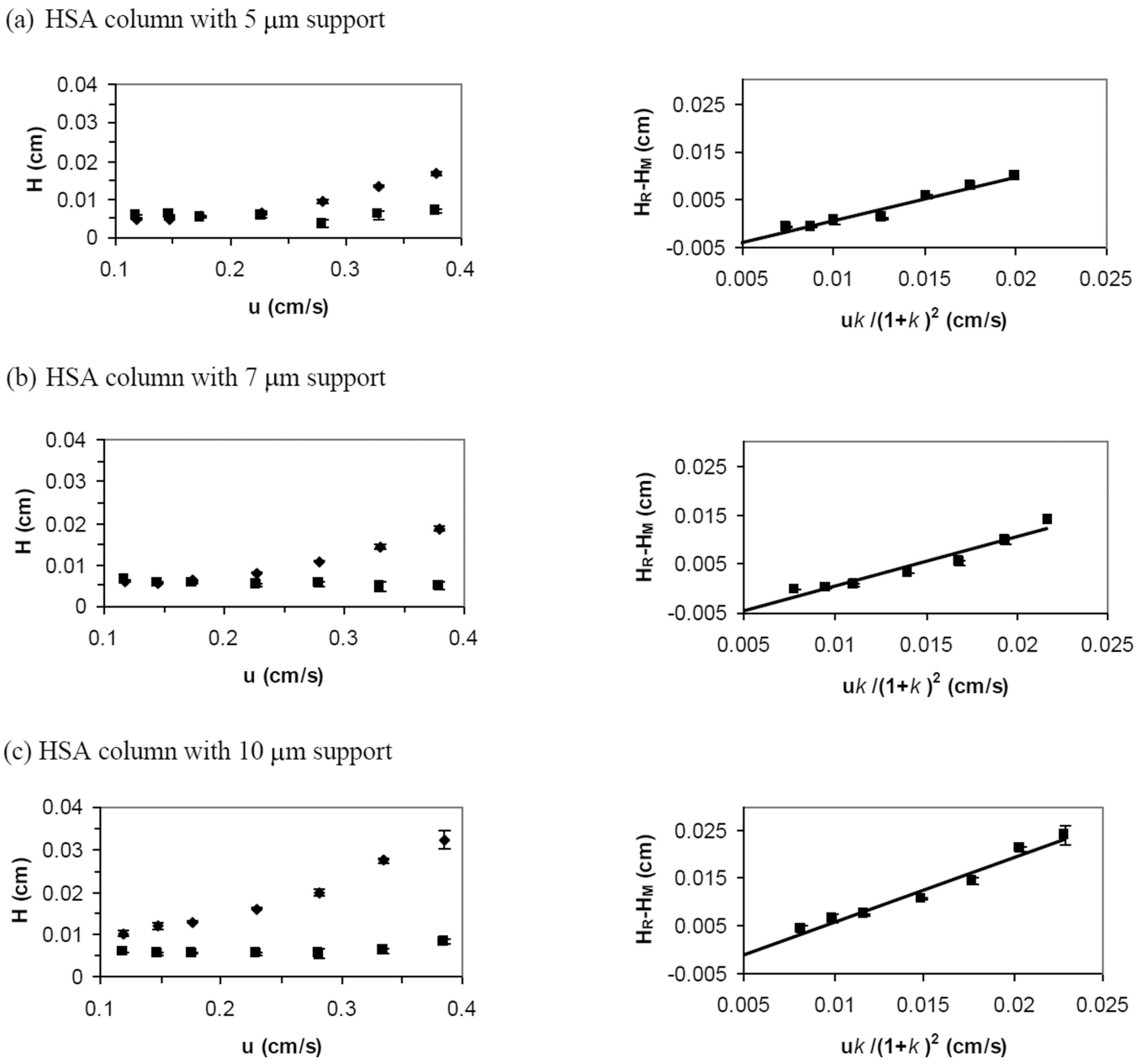

Figure 5.

Plate height curves (left) and plots of ($H_R - H_M$) versus (u k)/(1+k)^2 (right) obtained for HSA columns containing supports with particle diameters of (a) 5 μm, (b) 7 μm, or (c) 10 μm HSA columns. In the plate height curves, the total measured plate height for L-tryptophan (H_R) is represented by (◆) and the total measured plate height for sodium nitrate (H_M) is represented by (■). The best fit lines for the plots of ($H_R - H_M$) versus (u k)/(1+k)^2 were as follows: (a) y = 0.908 (± 0.086) x − 0.008 (± 0.001), (b) y = 1.009 (± 0.120) x − 0.010 (± 0.002), and (c) y = 1.362 (± 0.113) x − 0.008 (± 0.002), with correlation coefficients of 0.978, 0.966, and 0.983, respectively (n = 7). The error bars represent a range of ± 1 S.D. and are typically on the same size scale as the symbols used in these plots.

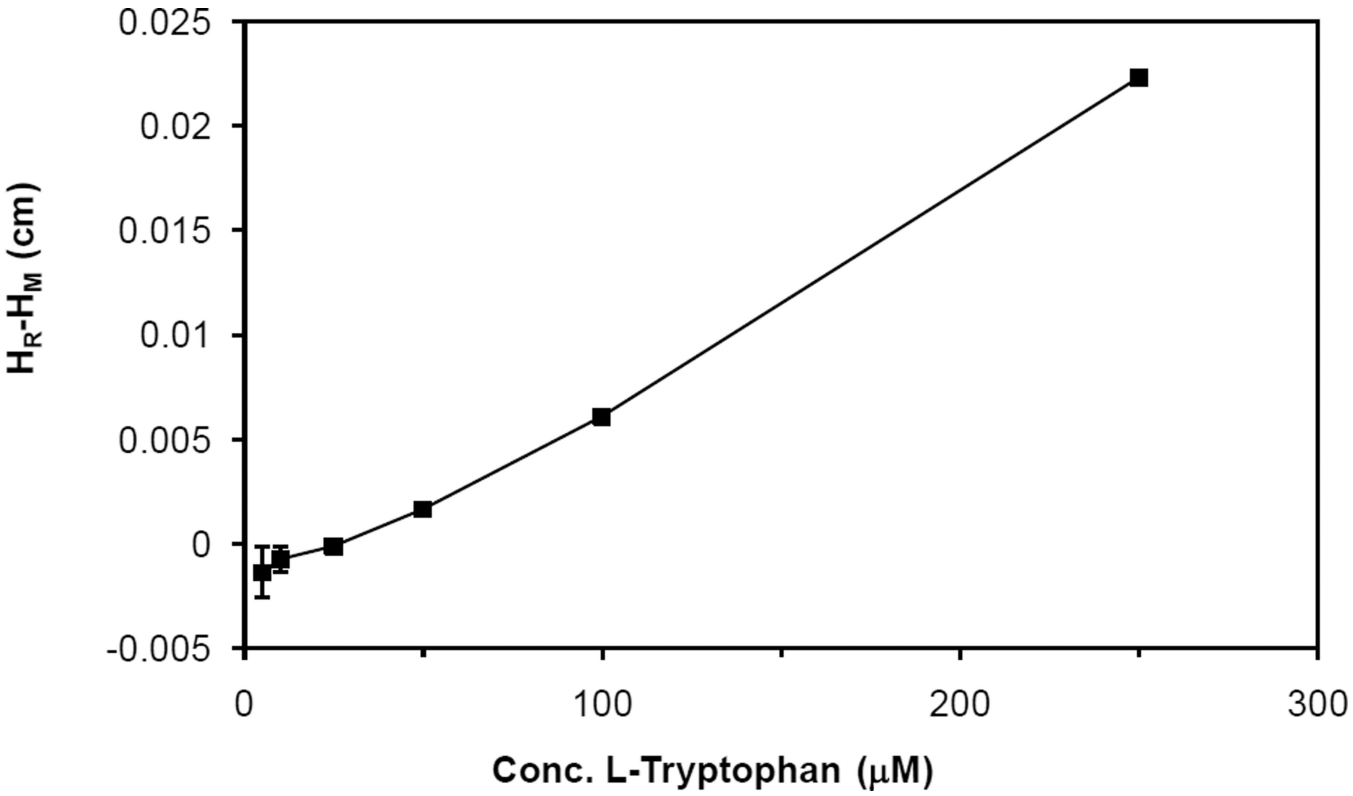

Figure 6.

Effect of sample concentration for L-tryptophan sample on the apparent value of ($H_R - H_M$). The concentration of sodium nitrate that was used to measure H_M in these studies was 25 μM. These results were obtained at 1.0 mL/min on an HSA column that contained a 5 μm diameter support. The error bars represent a range of ± 1 S.D.

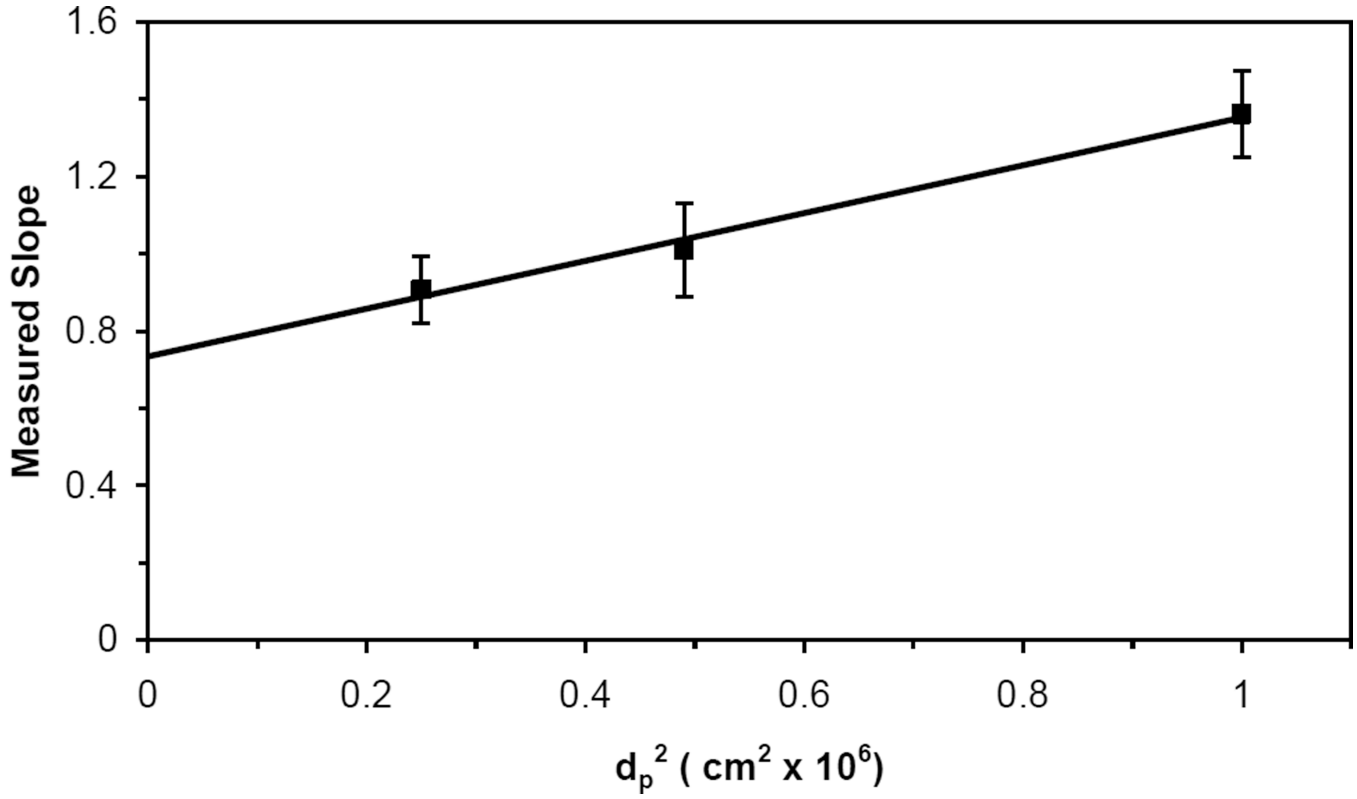

Figure 7.

Multi-column peak profiling graph for L-tryptophan, in which the slopes measured from the peak profiling plots in Figure 5 were plotted versus the square of the particle diameter of the support material within each column. The best fit line for this graph was y = 6.2 (± 0.7) x 10^5 x + 0.73 (± 0.04), with a correlation coefficient of 0.995 (n = 3). The error bars represent a range of ± 1 S.D.

Table 1

Dissociation rate constants determined using different peak profiling methods[a]

Measurement method	Type of HSA Support	Apparent k_d (s^{-1})
Peak profiling at a single flow rate (3.5 mL/min)[b]	10 μm Porous silica	1.9 (± 0.2)
	7 μm Porous silica	3.1 (± 0.1)
	5 μm Porous silica	4.1 (± 0.2)
Peak profiling at multiple flow rates (1.0–3.5 mL/min)[c]	10 μm Porous silica	1.5 (± 0.1)
	7 μm Porous silica	2.0 (± 0.2)
	5 μm Porous silica	2.2 (± 0.2)
Result extrapolated to d_p=0 using data from multiple columns[d]	N/A	2.7 (± 0.2)

[a] All of these results were obtained at 37°C in the presence of pH 7.4, 0.067 M phosphate buffer. The values in parentheses represent a range of ± 1 S.D.

[b] These dissociation rate constants were calculated by using eq 3.

[c] These dissociation rate constants were obtained by using eq 8.

[d] This result was obtained by using eq 10 and a plot of the slopes (from eq 9) for the multiple flow rate data versus d_p^2, where d_p is the particle diameter of the support material within each column.